WARWICK
THE UNIVERSITY OF WARWICK

Manuscript version: Author's Accepted Manuscript
The version presented in WRAP is the author's accepted manuscript and may differ from the published version or Version of Record.

Persistent WRAP URL:
http://wrap.warwick.ac.uk/163290

How to cite:
Please refer to published version for the most recent bibliographic citation information. If a published version is known of, the repository item page linked to above, will contain details on accessing it.

Copyright and reuse:
The Warwick Research Archive Portal (WRAP) makes this work by researchers of the University of Warwick available open access under the following conditions.

Copyright © and all moral rights to the version of the paper presented here belong to the individual author(s) and/or other copyright owners. To the extent reasonable and practicable the material made available in WRAP has been checked for eligibility before being made available.

Copies of full items can be used for personal research or study, educational, or not-for-profit purposes without prior permission or charge. Provided that the authors, title and full bibliographic details are credited, a hyperlink and/or URL is given for the original metadata page and the content is not changed in any way.

Publisher's statement:
Please refer to the repository item page, publisher's statement section, for further information.

For more information, please contact the WRAP Team at: wrap@warwick.ac.uk.

warwick.ac.uk/lib-publications

Local Characterization of Ferromagnetic Resonance in Bulk and Patterned Magnetic Materials using Scanning Microwave Microscopy

C. H. Joseph, Georg Gramse, Emanuela Proietti, Giovanni Maria Sardi, *Member, IEEE*, Gavin W. Morley, Ferry Kienberger, Giancarlo Bartolucci, Romolo Marcelli, *Member, IEEE*

***Abstract*—We have demonstrated the capabilities of the scanning microwave microscopy (SMM) technique for measuring ferromagnetic resonance (FMR) spectra in nanometric areas of magnetic samples. The technique is evaluated using three different samples, including an yttrium iron garnet (YIG) polycrystalline bulk sample and a thick YIG film grown by liquid phase epitaxy (LPE). Patterned permalloy (Py) micro-magnetic dots have been characterized to assess the performance for imaging applications of the technique, measuring the variation of the magnetic properties of the sample along its surface. The proposed technique may pave the way for the development of high spatially resolved mapping of magnetostatic modes in different nano and micro magnetic structures.**

***Index Terms*—Ferromagnetic resonance (FMR), Scanning Microwave Microscopy (SMM), Magnetostatic Modes, Yttrium Iron Garnet (YIG), Permalloy (Py).**

I. Introduction

THERE is currently a huge interest in the local properties of magnetic materials structured at the sub-micron or even at the nanometre level. In particular, shapes obtained by patterning techniques and exhibiting a low aspect ratio, like circular discs, ellipses and squares are suitable configurations for data storage [1] and spintronics [2] applications. They are simple building blocks but can be also viewed as model systems whose properties help in understanding complicated or more exotic micro and nanostructures. There are already a number of experimental and theoretical studies on the dynamic magnetic properties of arrays of dipole-coupled magnetic discs, with works dealing with the resonance frequency position with respect to the applied magnetic field [3], structure of the modes in the vortex state [4], and modes of excitation and their distribution for in-plane [5] and out-of-plane [6] applied DC magnetic fields. Identification of the spin-wave damping mechanisms has led to several studies into ferromagnetic resonance (FMR) linewidth broadening in such systems, including linear and nonlinear mechanisms. The possibility to perform imaging of FMR modes in these structures at GHz frequencies unlocked an important research opportunity for a full understanding of the mode excitation, especially in planar configurations based on the coupling between single resonating structures. The utilization of local characterization techniques, and possibly imaging based on near field measurements, leads to a complete definition of the planar electromagnetic mapping. So far, there are only a few contributions on FMR studies with near-field microwave techniques [7]–[12].

In this work, we report measurement data and discussion about local FMR detection on yttrium iron garnet (YIG) in bulk and film shapes, using microstrips to excite the magnetic material and detecting the resonance by using both a microstrip configuration and the probe of a near field scanning microwave microscope (SMM). Such a technique is particularly appealing for surface and sub-surface characterization of materials, even using a non-contact approach. It was extensively studied during the last decade with focus on its calibration [13]–[15], semiconductor properties [16]–[20], ferromagnetic materials [21] and detection of buried structures [22]. Other techniques, based on the evolution of the original AFM experiments, were also focused on calibration and quantitative analysis of local properties of materials, discussing in some detail the tip-material interaction [23]–[25].

It has to be pointed out that there have been strong efforts towards getting quantitative information from local characterization techniques, evidencing advantages and drawbacks of the developed setups, including the near field microwave microscopy, as discussed in [16], [26], [27]. Nevertheless, electromagnetic properties of materials, and especially their frequency response in the microwave range, need a purposely designed setup that is able to combine a typical scanning probe microscopy (SPM) resolution (below $1\,\mu m$) with high frequency capabilities. In fact, the materials studied in this

This research work was supported by the European Commission's Marie Curie PEOPLE-2012-ITN project: Microwave Nanotechnology for Semiconductor and Life Science "NANOMICROWAVE", under GA:317116. *(Corresponding author: Romolo Marcelli.)*

C. H. Joseph was with the National Research Council, Institute for Microelectronics and Microsystems (CNR-IMM), Via del Fosso del Cavaliere 100, 00133, Rome, Italy. He is now with the Department of Information Engineering, Università Politecnica delle Marche,Via Brecce Bianche, 60131 Ancona, Italy. (e-mail: h.j.christopher@staff.univpm.it)

Georg Gramse is with the Institute for Biophysics, Johannes Kepler University, Gruberstrasse 40, A-4020, Linz, Austria.

Emanuela Proietti, Giovanni Maria Sardi and Romolo Marcelli are with the National Research Council, Institute for Microelectronics and Microsystems (CNR-IMM), Via del Fosso del Cavaliere 100, 00133, Rome, Italy. (e-mail: romolo.marcelli@artov.imm.cnr.it).

Gavin W. Morley is with the Department of Physics, University of Warwick, Coventry CV4 7AL, UK.

Ferry Kienberger is with the Measurement and Research Lab, Keysight Technologies Austria GmbH, Gruberstrasse 40, A-4020, Linz, Austria.

Giancarlo Bartolucci is with the Department of Electronics Engineering, University of Rome "Tor Vergata", Via del Politecnico 1, 00133 Rome, Italy, and also with the National Research Council, Institute for Microelectronics and Microsystems (CNR-IMM), Via del Fosso del Cavaliere 100, 00133, Rome, Italy.

paper are magnetic ones with already established applications at microwave frequencies, but few works have been published about their local characterization, to study the shape of the resonance modes excited inside the material to eventually optimize the excitation in a device configuration. Other techniques devoted to the measurement of magnetic properties, like the magnetic force microscopy, are designed for DC or AC recording but not for studying the high frequency response of materials.

In this paper, magnetic garnet materials have been used for testing the sensitivity of the technique by measuring yttrium iron garnet (YIG) films grown by liquid phase epitaxy (LPE). Permalloy (Py) circular resonators have been also measured to check the resonance response as well as the imaging capabilities with high spatial resolution. Permalloy is used for several electronic applications, including FMR-driven high-speed transmission lines [28] or sensing [29]. Generally speaking, Py is chosen, like several other magnetic materials, including YIG, for magnetically tunable solutions [30], [31]. The proposed microwave microscopy approach may lead to a development of a tool for local FMR mapping with high spatial resolution as the setup is integrated with an atomic force microscopy (AFM) and the measurements are performed directly in the microwave regime by utilizing the higher dynamic range of the vector network analyzer (VNA). By modulating the magnetic field and selective detection of oscillating microwave response, we can surpress unwanted (capacitive) stray contribution and isolate the local FMR signal. A particularly convenient technique for local characterization, already developed by this group, was focused at the beginning on the modified arrangement of an AFM, namely an SMM developed by Keysight Technologies, using microwave signals to study material surface and sub-surface properties and with imaging capabilitites [32]. Because of the microwave nature of FMR, the SMM is particularly appealing for local characterization of magnetic resonance, and for this reason it has been used to extend the information coming out from resonance experiments, looking to the micro-scale excitation and not only to the overall device performance analysed by means of network analysis. The main contribution of this paper is the development of a local characterization technique for improving the understanding of the coupling between the microstrip transducers and magnetic garnet film resonators. Moreover, an alternative magnetic material like permalloy, also suitable of applications in microwave signal processing, has been studied with the same technique.

II. Background Theory

The ferromagnetic resonance phenomena are associated with the motion of magnetic dipoles in the presence of a constant DC magnetic field and a superimposed RF magnetic field [33]. The resonance arises when the energy levels of a quantized system of electronic or nuclear magnetic moments are split by the Zeeman effect due to the presence of a uniform magnetic field. An oscillating RF magnetic field causes an energy absorption at well-defined frequencies corresponding to the transitions between the levels. The classical situation is

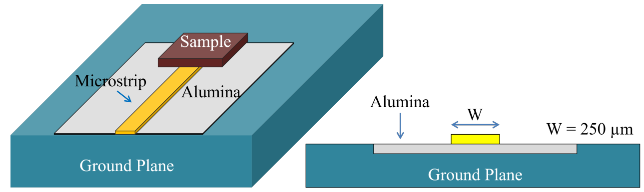

Fig. 1. Schematic diagram of the microstrip configuration.

well known and described in many papers and textbooks since the 1940's [33], [34], and recently reviewed, because of the increasing interest in small-size FMR experiments and their applications [35], [36].

In a simple model of a ferromagnetic system, the electron spins are characterized by a magnetic moment m, given by

$$m = -g\mu_B S \tag{1}$$

where g is the spectroscopic splitting factor, μ_B is the Bohr magneton (9.274×10^{-24}Am^2) and S is the spin. The magnetic moment is associated with an angular momentum, and it experiences a torque when it is in a static magnetic field H. This field can be an applied external DC field H_0 or the intrinsic anisotropy field H_A of the sample. As a result, the magnetization precesses around this field with angular frequency ω where,

$$\omega = \gamma H \tag{2}$$

Formally, the relationship between the resonance frequency, f, and the static magnetic field can be also expressed by

$$f = 2.8 \times 10^6 H \tag{3}$$

where f is in MHz and H is in Oe. g is related to the gyromagnetic ratio

$$\gamma = 1.76 \times 10^7 s^{-1} Oe^{-1} \tag{4}$$

A microwave magnetic field h can be superimposed to the static one and, using the complex notation, we can write that the sample will experience a total magnetic field

$$H = H_i + he^{j\omega t} \tag{5}$$

H_i is the sum of DC fields within the material, including the externally applied DC field H_0 and any time-independent internal field, i.e. demagnetization and anisotropy. Demagnetization is a shape dependent contribution, whereas anisotropy is mainly due to intrinsic properties of the material, often depending on the production technique. In formulae, we can write

$$\omega = \gamma H_i = \gamma(H_o - N_{demag} 4\pi M_S + H_A) \tag{6}$$

where N_{demag} is the demagnetizing factor, $4\pi M_S$ is the saturation magnetization of the material (temperature dependent) and $N_{demag}4\pi M_S$ is an internal field due to the presence of dipole moments induced on the surface, opposed to the external DC field. H_A is an anisotropy contribution, which is often oriented depending on the preferred direction induced

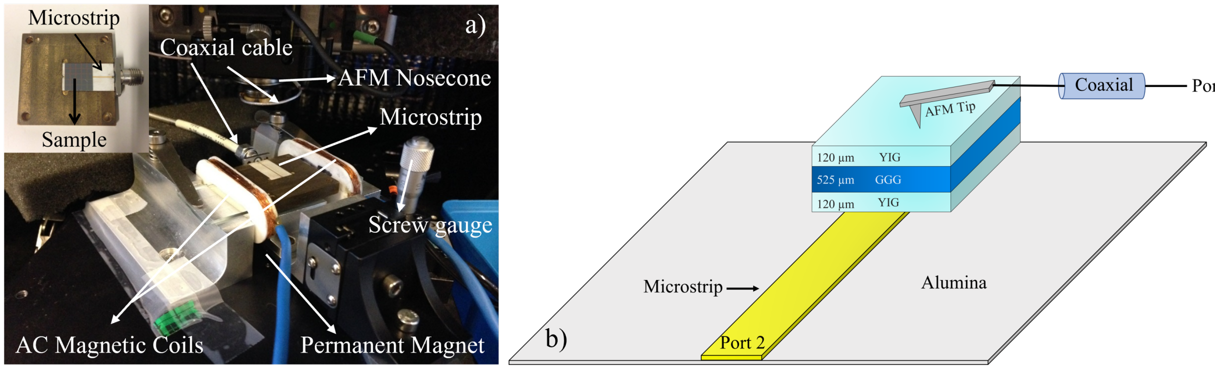

Fig. 2. (a) Photograph of the experimental arrangement. Inset shows the microstrip. (b) The schematic of two-port SMM measurement setup.

by the material growth (bulk crystal or film). The frequency-dependent field term, approximated by a plane wave, contains the amplitude h and the microwave frequency ω.

When the resonance condition is satisfied, i.e., the applied microwave frequency equals the natural precession frequency $\omega = \omega_0$, it is possible to transfer efficiently energy from the microwave field to the system of spins. When applying a constant external magnetic field along the z axis and an additional alternating field perpendicular to the DC field, at a frequency ω_0, the onset of an oscillation component of the torque, in phase with the precessional motion of the magnetic dipole is observed. Thus, the amplitude of the precession will grow and the energy will be absorbed from the applied microwave field. As outlined above, ω_0 depends on a number of factors such as the external magnetic field, the sample geometry, and the magneto-crystalline anisotropy. The applied magnetic field at resonance can be calculated if we know that the anisotropy contribution to the FMR frequency is negligible. In this case,

$$H_0 = 4\pi M_S + (\frac{2\pi}{\gamma})f \tag{7}$$

If the DC field is measured at the same time as the resonance frequency, the anisotropy can be analogously derived. For the case of pure YIG bulk samples or films (we used both for this study) and for negligible anisotropy contributions, we can write

$$H_0 = 1760 + \frac{f[MHz]}{2.8 \times 10^6} \tag{8}$$

Actually, $4\pi M_S = 1760\,Oe$ at room temperature for pure YIG samples.

III. Instrumentation and Materials

A. Experimental Setup

The commercial scanning microwave microscope (SMM) from Keysight Technology used for this experiment is composed of a standard 5600 atomic force microscopy (AFM) interfaced with a vector network analyzer (VNA). The VNA measures the full S-parameters (S_{ij} with $i = 1, 2$ and $j = 1, 2$) of a two-port network. In the proposed work, an unilateral configuration is used with port 1 and port 2 connected to the conductive AFM tip and to the transmission line (though a coaxial-to-microstrip transition) respectively.

The port 1 of the VNA is directly connected to the AFM tip through a coaxial transmission line. The port 2 is connected to a shorted microstrip antenna and the sample has been placed on top of the microstrip antenna (closer to the shorted end).

The microstrip is a planar transmission line, with a ground reference (metallization) on the back side of the substrate where it has been manufactured [37]. The concept of radiation impedance was introduced in past literature to calculate the electrical matching between the high frequency signal and the magnetic resonator, i.e. between the high frequency electromagnetic fields excited (radiated) in proximity of the metal sheets by the microwave current and the resonator [38]. In particular, the magnetic component exhibits circular lines around the direction of the high frequency signal, whereas the electric field is given by almost straight lines going from the microstrip plane to the ground, with the exception of the boundaries of the metal sheet, where a bending of the fields happens [39]. The magnetic resonator is placed on the top of the microstrip, and it is sensitive mainly to the magnetic lines of the microwave field, because of the validity of the magnetostatic approximation for a magnetic dielectric material. As a consequence, the Maxwell equations describing the resonance or the propagation are simplified and we can write them for the magnetic RF component only [30]. Alumina and silicon have been both used in the past to obtain microstrip or coplanar waveguide configurations used for exciting magnetic garnet film resonators [36]. Depending on how the microstrip is ended, i.e. loaded, opened or shorted, the microwave current flowing in the microstrip will be constant or can change with the distance from the termination. In our case we used a shorted line, and for this reason the maximum current will be at the end of the microstrip, with the first node occurring at $\lambda/4$ with respect to the short. The rule to have an almost homogeneous excitation of the magnetic film is to have its size l_y along the microstrip shorter than $\lambda/4(l_y < \lambda/4 = c/4f\sqrt{\varepsilon})$. In our case, the minimum frequency imposed for the experiment with the magnetic garnet films was around f = 5 GHz, and the dielectric constant of alumina is ε = 9.8; for the sample, we have $l_y = 4\,mm$. With these values, we have

$$\lambda/4 = 3 \times 10^{10}/(4 \times 5 \times 10^9 \times \sqrt{9.8})\,cm \approx 0.5\,cm \tag{9}$$

i.e. a value greater than the length of the resonator, thus providing a practically constant excitation of it. The smaller samples made by permalloy do not need a similar evaluation, because they are much smaller than the magnetic garnet resonator and smaller than any possible variation of the electromagnetic field within a size in order of tens of μm.

In Fig. 1 it is shown the shorted microstrip configuration. In this setup, port 2 was used for measuring the reflection coefficient of the magnetostatic wave device (one port resonator) whereas port 1 was used to record the transmission from the resonating device (excited with port 2) to the SMM tip. A NdIB (neodymium iron boron) permanent magnet is placed below the sample, and in this way a DC magnetic field is applied perpendicularly with respect to the sample surface; the variation of the magnetic bias is obtained by moving the magnet up and down below the sample plate using a manually adjustable micromanipulator. The photograph of the experimental arrangement is shown in Fig. 2(a). The same simple configuration has been used many times in the past to get narrowband filtering response of magnetostatic wave (MSW) devices, useful for notch filters [40], [41] as well as for feedback networks of tunable oscillators [42].

At the closest position of the permanent magnet to the sample surface, the maximum of the applied DC field is $\sim 0.4\,T$. The distance separation between the sample surface and the permanent magnet is in the order of $2\,mm$ at maximum for the lower values of the DC magnetic field, to guarantee the best homogeneity in the orientation of the DC magnetic field lines, vertically aligned with respect to the sample plane. Reproducibility in the experiment is obtained with a mechanical variation of the distance by means of a micrometric screw, readjusting the magnet position to have the same frequency of resonance and the same resonance shape when repeating the experience. In addition to the permanent magnet, two coils have been placed on the two sides of the sample plate to apply a modulated AC magnetic field parallel to the sample surface. The magnetic coils are then connected to the lock-in amplifier to provide a maximum voltage of $5\,V$ to the coils. This will produce AC magnetic fields in the order of few mT. Ports 1 and 2 are connected to the AFM tip and to the microstrip through a Dopant Profile Measurement Module (DPMM) arrangement, like the setup developed in [43], [44].

Analogously to the dC/dV measurement for obtaining the doping profile of semiconductor samples, here we measure the derivative of the signal with respect to the magnetic field (specifically, dS_{22}/dH or dS_{12}/dH), where S_{22} and S_{12} are the reflection and transmission scattering parameters recorded by means of the VNA. The amplitude and phase of the signal have both been measured. Once the sample is placed on the microstrip antenna, the values of the complex reflection coefficient S_{22} and of the transmission coefficient S_{12} are measured. S_{22} involves only the microstrip response. S_{12} involves both the SMM tip and the microstrip. In the latter case, the port 2 (microstrip) is excited with a microwave signal and the port 1 (SMM tip) will act as a receiver. The schematic representation of the two port arrangement is shown in Fig. 2(b). The VNA has been calibrated by imposing, as usual, the microwave power, the frequency sweep and the number of points for the frequency resolution within the chosen frequency range.

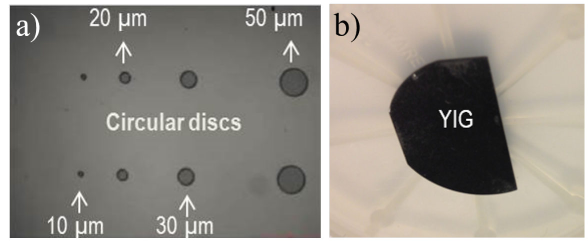

Fig. 3. (a) Optical micrograph of the patterned permalloy film structures. (b) YIG film sample grown by LPE technique.

The measurement of local properties of samples at the micro-to nano-scale involves signal levels that are quite low, and controlled boundary conditions are necessary to avoid vibrations and electromagnetic interferences. Moreover, especially for unknown or unexpected properties, like it is the case for materials exhibiting an electromagnetic response to a microwave excitation, it is important to check that the tip used for the measurements, which is a kind of microscopic antenna, does not suffer unwanted perturbations. It is worth noting that the measurement proposed in this paper is a characterization of a non-insertable device, because only on port 2 we have a connector, whose contribution can be de-embedded using a traditional calibration procedure. On the other side of the device is positioned a tip to be used as the receiving probe, and no commercial or well-established solution is available for calibrating both network analyzer ports with standard elements. This agrees with the specific goal of this work, where the detection of the electromagnetic field excited in a magnetic sample was measured, with the ambition for future experiments to map the entire mode of resonance for magnetic films excited by a high frequency signal. For the above reasons, preliminary tests have been performed on our peculiar arrangement to take under control cross-talk effects between the microstrip and the SMM tip. The signal level for the transmission on the air was measured as low as -30 dB, lower than the signal measured to detect the resonance of the YIG device. It has to be stressed that cross-talk is very low when it is measured on the air, and effective signals are measurable only when the sample is present, because of the contribution of the dielectric and magnetic properties of the media, i.e. the alumina substrate, the YIG film on the top or, in case of permalloy samples, silicon with a magnetic film deposited on it. In both measured configurations the separation between the microstrip and the SMM tip is greater than $500\,\mu m$. Additionally, differential measurements have been done for YIG samples using a classical approach for a resonance experiment, where a lock-in amplifier enhances the signal-to-noise ratio, giving back the derivative of the recorded signal with respect to the swept quantity, namely frequency or DC magnetic field. To distinguish the FMR peaks from possible spurious responses, two sweeps are necessary: the first one without applying any AC magnetic field from the coils and the second one by applying the AC magnetic field by means of the magnetic coils.

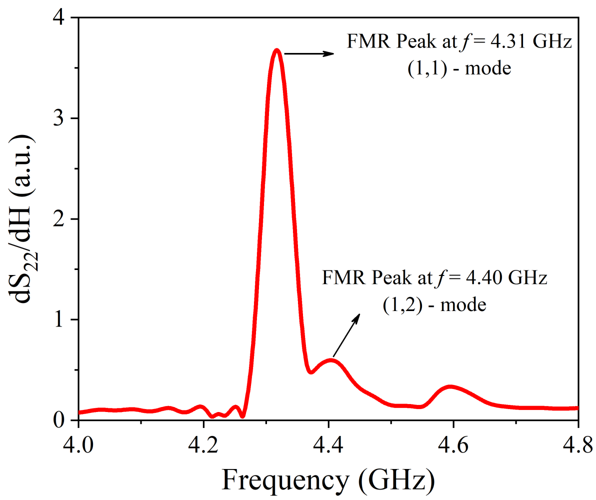

Fig. 4. FMR spectra of the YIG bulk sample obtained by subtracting the reference level for the reflection case S_{22}.

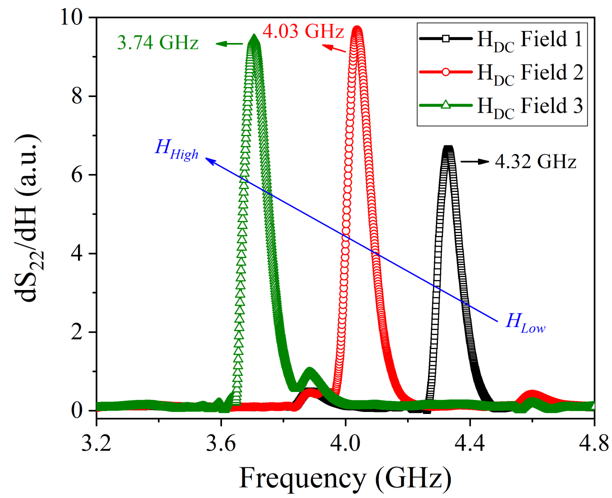

Fig. 5. FMR spectra of the YIG bulk sample with respect to different H_{DC} fields.

B. Samples Preparation

Three different kinds of samples are considered for the characterization. First, spectroscopic measurements (resonance signals) have been recorded for a YIG bulk and for a liquid phase epitaxy (LPE) grown film. Then, patterned micro-structures of permalloy (Py) have been measured using both spectroscopic and imaging capabilities of the experimental setup.

The YIG film sample has been grown by LPE on a gadolinium gallium garnet (GGG) substrate $< 111 >$ oriented and presents a thickness of $\sim 120\,\mu m$ on both sides of the GGG substrate. The bulk YIG is a (5×5 mm^2) square sample grown by chemical vapour deposition (CVD) with a thickness of $\sim 500\,\mu m$.

The Py microstructures are disks obtained by thermal evaporation of a $50\,nm$ film, and the circles defined by standard photolithographic mask sequence process to obtain 10, 20, 30 and 50 μm as a diameter on a 4-inch high-resistivity silicon wafer having a thickness of 300 μm. The use of low-resistivity silicon wafer substrates has been avoided in the fabrication, to suppress the onset of the eddy currents contribution in the substrate during measurements. The distance imposed between the circular dots is triple with respect to the diameters. As a result, the magnetic dipole interaction between the dots is negligible. This enables measurements of the response coming only from a single structure, but not the collective response or any other interaction which comes from the neighboring structures. The prepared Py microstructures and the YIG samples are shown in Fig. 3 (a) and (b).

IV. Results and Discussion

A. Spectroscopic Measurements

The first measurements have been performed with the bulk YIG sample as it is very homogenous and thick, and it shows a good electrical coupling with the microstrip antenna. The port 2 of the VNA provided the microwave excitation to the microstrip line, and the measurement of the reflection parameter S_{22} has been recorded. In the classical FMR experiments, with a resonance cavity loaded by a small sample, the excitation frequency is fixed, and the applied DC magnetic field is varied until the resonance occurs. In our experiment, following a tradition in the determination of the material properties as a function of frequency [45], we fixed the H_{DC} field (fixing the position of the permanent magnet) and the frequency has been swept. This approach agrees with the most part of the recent experiments devoted to the necessity to sweep the frequency in applications where magnetic materials are used for tunable devices or for updated techniques based on the frequency sweep [46].

All the measurements are performed between 1 GHz and 10 GHz. The static magnetic field was applied perpendicular to the surface of the sample with the permanent magnet, and it was strong enough to saturate the sample: the magnetization was less than half of the applied DC field. Initially, we measured the reflection (S_{22}) alone considering only the microstrip. In this case, the FMR signal is expected to be high, because an electrically matched and shorted microstrip is directly coupled to the exploited sample, in an area with the maximum available RF power, i.e. close to the short.

Fig. 4 shows the FMR spectra for the bulk YIG sample in the microstrip reflection measurement arrangement. When no AC magnetic field is applied, the FMR peak detected by the lock-in is absent, and only spurious resonances are seen which are induced by the equivalent circuit coming from the dielectric contributions of the setup. This can be considered a cumulative effect due to the materials, e.g. YIG and GGG, as well as to the cables and other details of the experimental setup. When the modulated AC magnetic field is applied, the FMR peak of the fundamental mode appears. The spectra obtained without AC magnetic field has been taken as a reference level. The FMR peak is detected at 4.31 GHz. Using the simple equations (7) and (8) introduced in the theory of the ferromagnetic resonance, one can calculate the applied magnetic field from the FMR frequency value and vice versa. Using this approximation (8), i.e. neglecting the

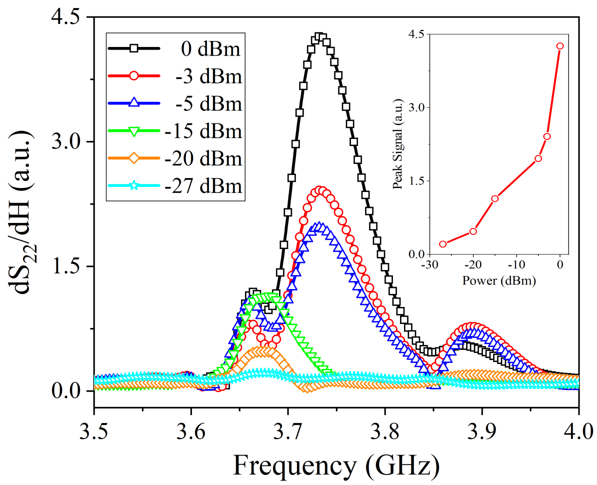

Fig. 6. FMR spectra of the YIG bulk sample with respect to different values of the microwave power.

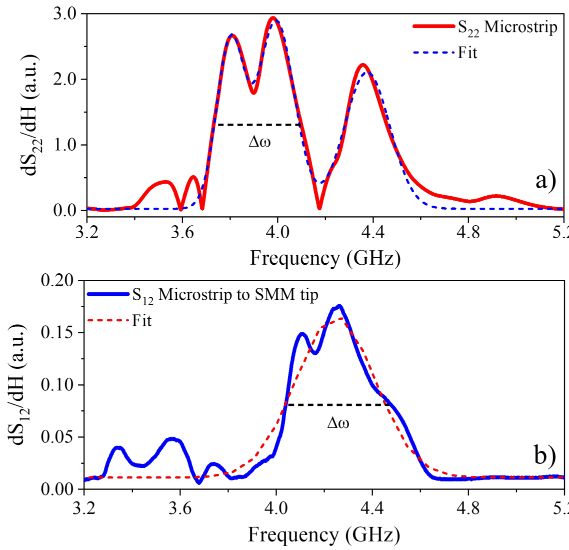

Fig. 7. FMR spectra of the YIG film sample. (a) The reflection spectrum S_{22} and its multiple peak fit. (b) The transmission spectrum S_{12} and its fit analysis.

anisotropy, which in most cases is not larger than 1/10 of the saturation magnetization, the static field applied to the sample is around 3300 Gauss. The FMR peak is clearly sensitive to the DC magnetic bias value, and the FMR frequency moved to lower values when the DC magnetic field is decreased, as expected from the almost proportionality between frequency of resonance and the applied DC field.

It is worth noting that when the magnetic field is varied from 3300 Gauss to 3000 Gauss, then the FMR frequency shifted from 4.32 GHz to 3.70 GHz, as it is shown in Fig. 5. The equations defined in the section about the theory of magnetostatic wave excitation have been used to determine the expected frequency range for the onset of the resonance modes. First, the static field generated by the permanent magnet was measured considering the position with respect to the material under test, and successively the frequency range evaluated according to the theory. The agreement is within 100 MHz, thus allowing to neglect the anisotropy contribution and to guide us efficiently in the frequency range to be imposed for the experiment. The linewidth, i.e. the width of the resonance curve at half amplitude, does not change with the change in the external field. Actually, it is expected that the material losses are slightly dependent on the frequency in a narrow range. The linewidth, i.e. the width of the resonance curve at half amplitude, does not change with the change in the external field. Actually, it is expected that the material losses are slightly dependent on the frequency in a narrow range.

In order to check for nonlinearities, the power of the applied microwave field has been also swept, while maintaining the DC magnetic field constant. The peak started to get damped when going to very low powers. Actually, the power varied from 0 dBm to -27 dBm, and the peak disappears at -27 dBm, as it is shown in Fig.6. The response is always linear, as to observe nonlinear effects like peak broadening or distortions more power is needed. The inset shows that increase in the amplitude of the FMR peak is consistent with the increase of the input power because an absolute value and not a relative one is measured.

The next set of experiments are carried out with the YIG thick film sample grown by LPE technique. The microwave excitation is provided at the port 2, which is connected to the microstrip and on top of the sample the transmitted signal is measured with the AFM tip of the SMM and recorded at port 1. The tip is placed in the middle of the resonator because the main mode will have a maximum there, coherently with the position of the microstrip for the bottom film, which is normally characterized by maxima in the center and nodes on the edges, ignoring corrections due to an exact knowledge of the boundary conditions. In Fig. 7 the comparison between the reflection and the transmission of the FMR spectra is shown.

Two differences with respect to the previous experiment on bulk YIG have to be noticed. First of all, the best coupling is obtained with the microstrip measurement, because the sensing volume is much higher and the electrical matching (50-ohm condition) is provided by a typical resonator device configuration, and for this reason the highest signal is obtained with measurements performed on the bottom film, i.e. with the one placed in direct contact with the microstrip. In this case, as evidenced from Fig. 2(b), a number of modes are also excited, because of the finite width of the resonator (the planar size is $2.5 \times 4\, mm^2$). For the above reasons, the coupling is poor for the top film, because it is far from the microstrip exciting the microwave signal at least for a distance equal to $120 + 525 = 645\, \mu m$, i.e., the bottom YIG film plus the GGG substrate. Moreover, the detection of the signal is performed by means of the SMM tip, which is not electrically matched as the microstrip. This results in a transmission signal that is weaker than the reflected one by a factor of 1/10 or less.

No coupling effects between the two YIG films have to be considered, because the distance between them is large enough to eliminate these effects. To have an order of magnitude for the signal decay from the microstrip to the top film, we can consider that the main (1,1) mode corresponds to a wave-

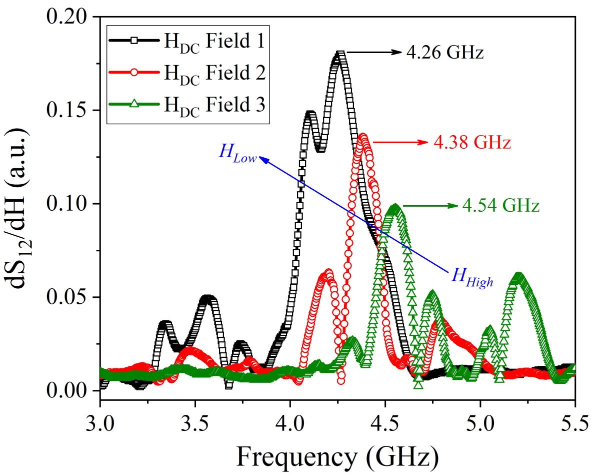

Fig. 8. FMR transmission spectra of the YIG top film with different H_{DC} fields.

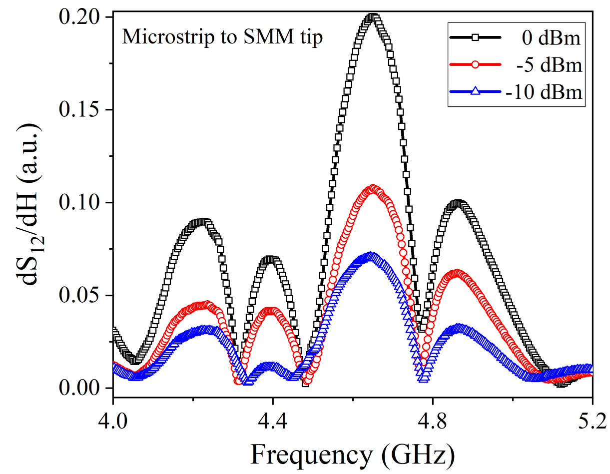

Fig. 9. FMR spectra of the YIG film for different microwave power levels.

vector value given by

$$k_{1,1} = \pi\sqrt{\left[(\frac{1}{l_x})^2 + (\frac{1}{l_y})^2\right]} \tag{10}$$

In our case, the sample dimensions are $l_x = 2.5\,mm$ and $l_y = 4\,mm$. Then, the value of the wave-vector for the fundamental mode is $k_{1,1} \approx 14.8\,cm^{-1}$. The scalar potential for the excited magnetostatic wave decays outside the film with an exponential law, and the corresponding absorbed power is a function of the square of the magnetic field h, calculated with its components $h_x = \mathrm{d}\psi/\mathrm{d}x$ and $h_y = \mathrm{d}\psi/\mathrm{d}y$, which is oscillating in the plane and decaying along z. Then, the power outside the YIG film goes like $\exp(-2zk_{1,1})$, where z is the distance from the microstrip plane. At $z = 645\,\mu m = 0.0645\,cm$, the decay of the signal will be evaluated by means of the expression, $\exp(-2 \times 0.0645 \times 14.8) \approx 0.15$.

Looking to Fig. 7, the ratio between the measured voltages at the FMR peak for the reflection and for the transmission case is given by $S_{22}/S_{12} \sim 0.06$. This actually means that the lowering of the peak is due, almost in equal measure, to both decay of the signal and un-matching for the SMM tip.

The line width $\Delta\omega$ (width at half amplitude) obtained by means of the two measurements (reflection and transmission) has also been checked by fitting the FMR peaks. The small shift between the frequency of resonance for the two cases is reasonably due to the small difference of the magnetic field for the top film with respect to the bottom one, being the two films positioned in a different place inside the DC bias magnetic field. The fitted reflection case is characterized by a linewidth $\Delta\omega_R = 424$ MHz in Fig. 7(a) and the transmission case by $\Delta\omega_T = 387$ MHz in Fig. 7(b). The small difference between the two inferred values for the linewidth can be considered acceptable. It is in the order of 10% and it is obtained from two different measurement approaches, characterized also by a different sensitivity and mode excitation. Owing to the best coupling experienced for the microstrip experiment, the main mode is excited efficiently, while the high order ones are depressed. In the case of the SMM detection, the AC field generated by the microstrip is not immediately coupled to the magnetic film on the top surface, and this configuration introduces some inhomogeneity in the region of interaction, enhancing high order modes with respect to the main one. Since the modes excited in the last configuration are very close to the main natural one, the linewidth does not suffer any frequency dependence and it is almost the same.

Actually, in Fig. 7(b) the response of the top film shows that the main mode at higher frequency has been suppressed, and two higher order modes are partially overlapped. As discussed above, Fig. 7(b) shows the FMR spectrum for the YIG top film, measured with the SMM tip. The resonance appears at 4.26 GHz, when the external static magnetic field value is $H_{DC} \sim 3281$ Gauss. FMR spectra have been recorded for different magnetic field values and the results for the transmission parameter are shown in Fig. 8. Observing from Fig. 8, it is evident that the resonance of patterned micro-magnetic structures is not exactly rigidly shifted by changing the bias magnetic field. This can be understood, analogously with the excitation of MSW modes, considering the complex relationship linking the electrical matching with the film geometry and the electromagnetic boundary conditions. Only using specific precautions, a selected mode can be tuned by means of the bias, otherwise the microstrip alone is a source of not homogeneously excited modes, including even and odd ones, and the best coupled modes can change by changing the bias.A power sweep measurement has been also performed and looking to the lock-in signal the resonance peak is damped when decreasing the power levels, as it is shown in Fig. 9.

The reason for the setup proposed in this resonance experiment, including the transmission case, is the future possibility to map the local electromagnetic field distribution of the excited mode, using both spectroscopy and imaging capabilities of the near-field microwave measurement. For the YIG film case, it was not possible to image the modes, as the sample area is much bigger than the scanning limitation of the SMM, but it is interesting and promising to image smaller confined magnetic structures.

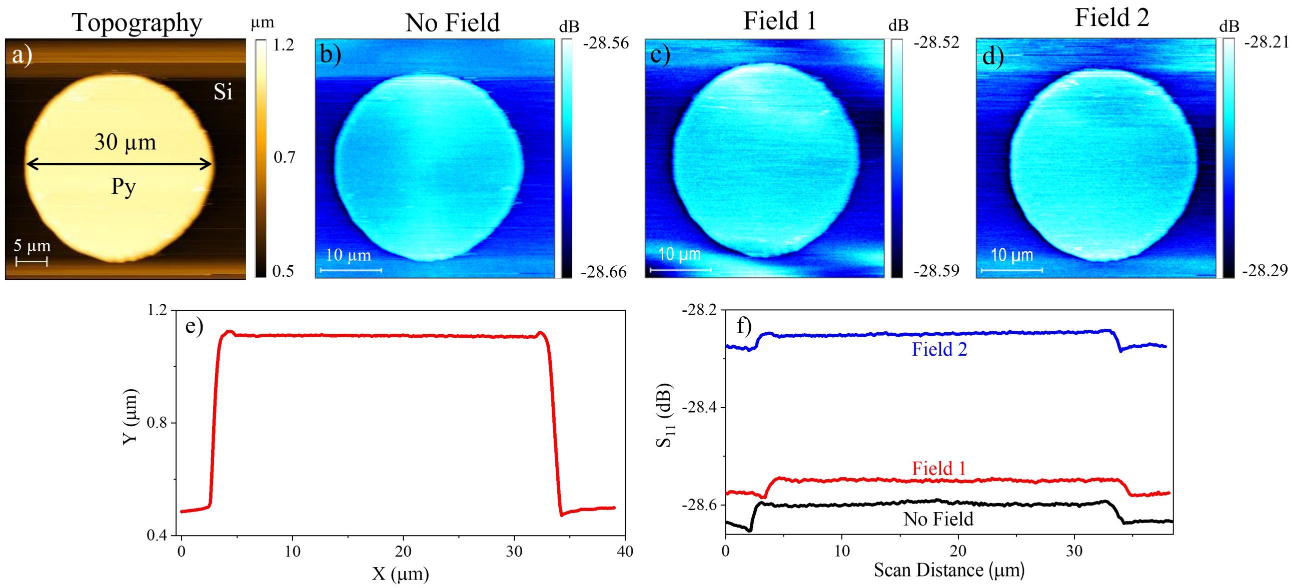

Fig. 10. SMM images of the patterned 30 μm Py circle (a) Topography, (b) SMM amplitude image at zero DC magnetic bias, (c) Amplitude image with applied DC magnetic bias value of 1.15 kOe (field 1), (d) Amplitude image with increased DC magnetic bias of 1.87 kOe (field 2), (e) Topography profile, (f) The profiles taken at the center of the SMM amplitude images using the reflection parameter S_{11}.

B. Patterned Micromagnetic Structures

The SMM measurements considering both imaging and spectroscopy aspects have been performed on the patterned Py layer deposited onto a silicon wafer, as detailed in the sample preparation section. The measurements have been done on 30 μm and 50 μm diameter circles for obtaining topographic and microwave data, to give evidence for the magnetic DC bias effects on both imaging and spectroscopic response of the structures. The frequency has been swept initially from 1 GHz to 20 GHz, and we recorded simultaneously the AFM topography and VNA amplitude as well as phase data for the 30 μm circle at 19.13 GHz. In experiments performed on Py circles, port 1 of the VNA was used to launch the signal, as only reflection measurements have been recorded.

The same data have been recorded for two different external DC magnetic field variations. In Fig. 10 the images recorded are shown. Fig. 10 (a) and (e) shows the topography and its line profile taken at the center of the image, along the diameter. When varying the external magnetic field by changing the DC magnet position below the sample in the developed setup, the reflected microwave signal is changing and this can be attributed to the alteration of the magnetic properties of the sample depending on the applied external magnetic field. Fig.10 (b), (c) and (d) shows the SMM amplitude images for no applied DC magnetic field case, as well as for two different magnetic bias values. From the line profiles that are shown in Fig. 10 (f), the variation is clearly visible. Actually, the topography remains constant, as the shape of the curve showing the profile is unchanged, but the amplitude for the S_{11} parameter exhibits a modification of the microwave response of the sample when increasing the magnetic bias. This can be interpreted in terms of the progressive alignment of the spins in the direction of the DC magnetic field when it is increased, contributing to the magnetic saturation of the sample, the onset of a single domain structure and, consequently, the decrease of magnetic losses due to the presence of magnetic domains.

Actually, as known from classic literature, the spin wave is affected by higher losses in the propagation when it passes through multiple domain walls; the full magnetic saturation of the sample imposes a single domain configuration with lower spin wave losses, condition that is fulfilled when the DC magnetic field overcomes the threshold of (4/3) the saturation magnetization, which is actually the case for the H-fields used in this work. This clarifies the capability of the developed setup in sensing the external DC magnetic field variation on the sample surface with the SMM tip.

Additional local FMR has been performed on the 50 μm wide Py circle. In order to identify the FMR resonance, the frequency has been swept from 7 GHz to 10 GHz and the FMR peak for the transmission case is detected by the SMM tip at around 9.2 GHz. The imaging of the Py disk was performed at a single frequency of 9.25 GHz where the FMR peak appeared. The resulting images are shown in Fig. 11. Although the signal-to-noise ratio of the shown S_{12} amplitude and phase was lower for the thin patterned Py film compared to the bulk and thick YIG film samples, still the FMR signal is detected for the transmission case on the Py sample. This is shown in the Fig. 11 (d), where we display a frequency sweep of the dS_{12}/dH signal together with the reference signal where no AC magnetic field is applied. The FMR peak is shifting to lower frequency when lowering the DC magnetic bias from 2.3 kOe to 1.8 kOe as shown in Fig. 11 (e). When reducing the microwave power, the FMR signal strength gets lowered and disappeared completely at -10 dBm of applied power. Fig. 11 (f) shows the FMR strength as a function of applied microwave power. However, further improvement of the signal-to-noise ratio is necessary for locally mapping the different FMR modes on the surface of the Py magnetic dot.

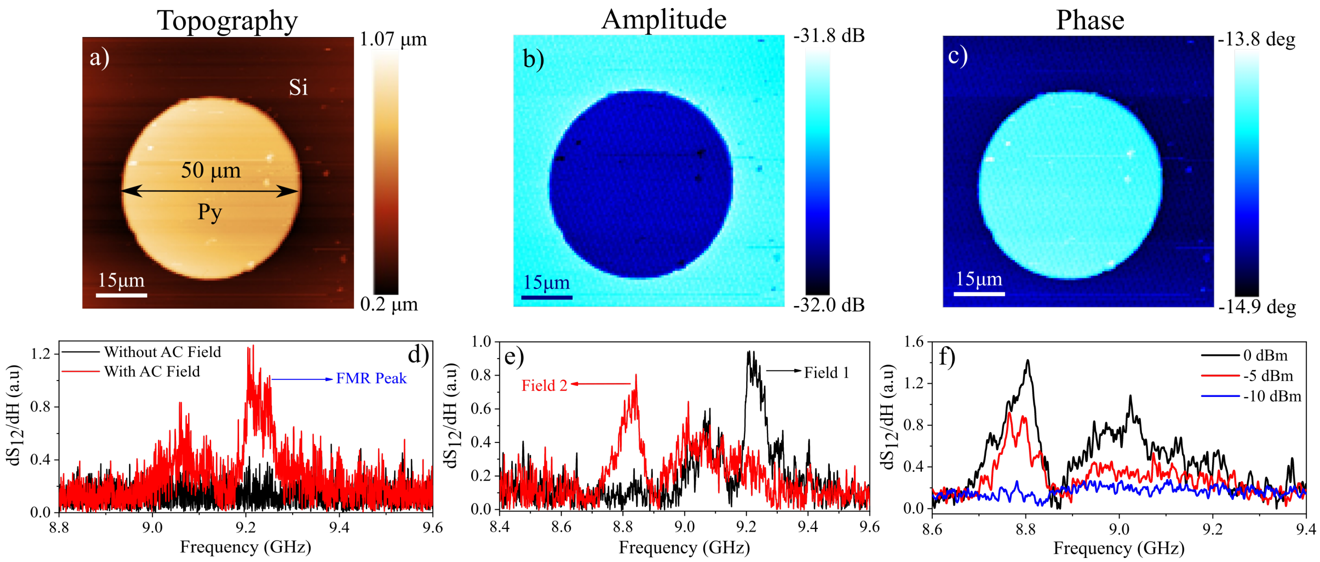

Fig. 11. SMM images of the patterned 50 μm Py circle. (a) Topography, (b) SMM amplitude, (c) SMM phase (d) FMR signal with the reference signal, (e) Shift of FMR peaks with respect to two different DC magnetic bias values of 2.3 kOe (field 1) and 1.8 kOe (field 2), (f) FMR signal with different microwave power levels.

Micro- to nano-scale measurements require a very high sensitivity giving a still sufficient signal-to-noise ratio to detect information of the material that can be easily processed. The smaller the SMM probe the higher is of course the lateral resolution, but the lower is the electrical sensitivity. Since the SMM operates in contact mode, tip wearing leads to a slight increase of the initial probe size during measurements. While this has a positive effect on the S/N, the probe has to be replaced at the due time if lateral resolution is of priority [20], [47]. In the measurements presented in this paper problemthe probe size influence could be related only with the characterization of the permalloy disks, measured by scanning the surface of samples as it is shown in Fig. 10 and Fig. 11. The change of the measured S-parameter with the applied DC field is quite small, but measurable. On the other hand, looking to [20], the wearing effect is typically smaller than the results of our measurements, thus demonstrating that the changes shown in both the above cited figures are due to the modification of the magnetic response of the sample and not to the tip wearing. Moreover, we want to point out that tips were changed after a few measurements, to avoid serious artifacts in the reproducibility of the results. Concerning the magnetic garnet resonators, they were measured without scanning, but just positioning the tip in the center of the sample, where the excited main resonance mode is expected to present a maximum, and in this case no wearing effect needs to be considered.

V. Conclusion

We have demonstrated the capabilities of the developed SMM-FMR setup for the detection of local FMR excitations using bulk and thin patterned magnetic samples. Both reflection and transmission cases were used to detect the FMR signals, giving complementary information about mode excitation and linewidth of the investigated material. The obtained spectroscopic measurements on the thick YIG film sample evidenced a weaker coupling at the nanometric SMM tip over 645 μm of sample thickness excited from the bottom, but it is still able to detect the FMR signal. Patterned Py magnetic dots have been imaged and the FMR spectrum has been measured. Although a local FMR signal could be clearly detected, an enhancement of the signal-to-noise ratio is still required for mapping the FMR modes in the nano-magnetic structures for basic understanding of the local FMR, but also for many future applications based on the local resonance. Actually, as any other local technique, even the detection of magnetic inclusions and imperfections can help to test the local homogeneity of the material as well as the microwave response of arrays based on micro- and nano-structures.

VI. Acknowledgment

Dr. Pavel Kabos from NIST Boulder, CO (USA) is kindly acknowledged for helpful scientific discussions on this topic during the above-mentioned project and the follow-up of the activity.

References

[1] B. D. Terris and T. Thomson, "Nanofabricated and self-assembled magnetic structures as data storage media," *Journal of Physics D: Applied Physics*, vol. 38, no. 12, pp. R199–R222, Jun 2005.

[2] S. I. Kiselev, J. C. Sankey, I. N. Krivorotov, N. C. Emley, R. J. Schoelkopf, R. A. Buhrman, and D. C. Ralph, "Microwave oscillations of a nanomagnet driven by a spin-polarized current," *Nature*, vol. 425, pp. 380–383, May 2003.

[3] G. N. Kakazei, Y. G. Pogorelov, M. D. Costa, T. Mewes, P. E. Wigen, P. C. Hammel, V. O. Golub, T. Okuno, and V. Novosad, "Origin of fourfold anisotropy in square lattices of circular ferromagnetic dots," *Phys. Rev. B*, vol. 74, p. 060406, Aug 2006.

[4] J. Shibata and Y. Otani, "Magnetic vortex dynamics in a two-dimensional square lattice of ferromagnetic nanodisks," *Phys. Rev. B*, vol. 70, p. 012404, Jul 2004.

[5] J. Jorzick, S. O. Demokritov, B. Hillebrands, B. Bartenlian, C. Chappert, D. Decanini, F. Rousseaux, and E. Cambril, "Spin-wave quantization and dynamic coupling in micron-size circular magnetic dots," *Applied Physics Letters*, vol. 75, no. 24, pp. 3859–3861, Jun 1999.

[6] G. N. Kakazei, P. E. Wigen, K. Y. Guslienko, V. Novosad, A. N. Slavin, V. O. Golub, N. A. Lesnik, and Y. Otani, "Spin-wave spectra of perpendicularly magnetized circular submicron dot arrays," *Applied Physics Letters*, vol. 85, no. 3, pp. 443–445, Jul 2004.

[7] T. An, N. Ohnishi, T. Eguchi, Y. Hasegawa, and P. Kabos, "Local excitation of ferromagnetic resonance and its spatially resolved detection with an open-ended radio-frequency probe," *IEEE Magnetics Letters*, vol. 1, pp. 3 500 104–3 500 104, Feb 2010.

[8] R. Joffe, E. Kamenetskii, and R. Shavit, "Near-field microwave microscopy based on ferrite disk sensors with magnetostatic resonances," in *44th European Microwave Conference*, 2014, pp. 291–294.

[9] R. Joffe, R. Shavit, and E. Kamenetskii, "Multiresonance measurement method for microwave microscopy," *IEEE Transactions on Instrumentation and Measurement*, vol. 66, no. 8, pp. 2174–2180, Mar 2017.

[10] S. Tamaru, J. A. Bain, R. J. M. van de Veerdonk, T. M. Crawford, M. Covington, and M. H. Kryder, "Imaging of quantized magnetostatic modes using spatially resolved ferromagnetic resonance," *Journal of Applied Physics*, vol. 91, no. 10, pp. 8034–8036, May 2002.

[11] C. Long, N. Taketoshi, H. Yang, and I. Takeuchi, "Development of a scanning probe microscope for localized ferromagnetic resonance measurements," in *APS March Meeting*, vol. 54, no. 1, 2009.

[12] D. I. Mircea and T. W. Clinton, "Near-field microwave probe for local ferromagnetic resonance characterization," *Applied Physics Letters*, vol. 90, no. 14, p. 142504, May 2007.

[13] M. Farina, D. Mencarelli, A. Di Donato, G. Venanzoni, and A. Morini, "Calibration protocol for broadband near-field microwave microscopy," *IEEE Transactions on Microwave Theory and Techniques*, vol. 59, no. 10, pp. 2769–2776, Aug 2011.

[14] G. Gramse, M. Kasper, L. Fumagalli, G. Gomila, P. Hinterdorfer, and F. Kienberger, "Calibrated complex impedance and permittivity measurements with scanning microwave microscopy," *Nanotechnology*, vol. 25, no. 14, p. 145703, Mar 2014.

[15] T. Dargent, K. Haddadi, T. Lasri, N. Clément, D. Ducatteau, B. Legrand, H. Tanbakuchi, and D. Theron, "An interferometric scanning microwave microscope and calibration method for sub-ff microwave measurements," *Review of Scientific Instruments*, vol. 84, no. 12, p. 123705, Dec 2013.

[16] A. Karbassi, D. Ruf, A. D. Bettermann, C. A. Paulson, D. W. van der Weide, H. Tanbakuchi, and R. Stancliff, "Quantitative scanning near-field microwave microscopy for thin film dielectric constant measurement," *Review of Scientific Instruments*, vol. 79, no. 9, p. 094706, Sep 2008.

[17] S. S. Tuca, M. Kasper, F. Kienberger, and G. Gramse, "Interferometer scanning microwave microscopy: Performance evaluation," *IEEE Transactions on Nanotechnology*, vol. 16, no. 6, pp. 991–998, Aug 2017.

[18] H. P. Huber, M. Moertelmaier, T. M. Wallis, C. J. Chiang, M. Hochleitner, A. Imtiaz, Y. J. Oh, K. Schilcher, M. Dieudonne, J. Smoliner, P. Hinterdorfer, S. J. Rosner, H. Tanbakuchi, P. Kabos, and F. Kienberger, "Calibrated nanoscale capacitance measurements using a scanning microwave microscope," *Review of Scientific Instruments*, vol. 81, no. 11, p. 113701, Nov 2010.

[19] J. A. Morán-Meza, A. Delvallée, D. Allal, and F. Piquemal, "A substitution method for nanoscale capacitance calibration using scanning microwave microscopy," *Measurement Science and Technology*, vol. 31, no. 7, p. 074009, Apr 2020.

[20] L. Michalas, F. Wang, C. Brillard, N. Chevalier, J. M. Hartmann, R. Marcelli, and D. Theron, "Modeling and de-embedding the interferometric scanning microwave microscopy by means of dopant profile calibration," *Applied Physics Letters*, vol. 107, no. 22, p. 223102, Dec 2015.

[21] C. H. Joseph, G. M. Sardi, S. S. Tuca, G. Gramse, A. Lucibello, E. Proietti, F. Kienberger, and R. Marcelli, "Scanning microwave microscopy technique for nanoscale characterization of magnetic materials," *Journal of Magnetism and Magnetic Materials*, vol. 420, pp. 62–69, Dec 2016.

[22] A. Lucibello, G. M. Sardi, G. Capoccia, E. Proietti, R. Marcelli, M. Kasper, G. Gramse, and F. Kienberger, "A broadband toolbox for scanning microwave microscopy transmission measurements," *Review of Scientific Instruments*, vol. 87, no. 5, p. 053701, May 2016.

[23] G. M. Sacha, E. Sahagún, and J. J. Sáenz, "A method for calculating capacitances and electrostatic forces in atomic force microscopy," *Journal of Applied Physics*, vol. 101, no. 2, p. 024310, Jan 2007.

[24] Z. Wei, Y. T. Cui, E. Y. Ma, S. Johnston, Y. Yang, R. Chen, M. Kelly, Z. X. Shen, and X. Chen, "Quantitative theory for probe-sample interaction with inhomogeneous perturbation in near-field scanning microwave microscopy," *IEEE Transactions on Microwave Theory and Techniques*, vol. 64, no. 5, pp. 1402–1408, Mar 2016.

[25] G. M. Sacha, "Method to calculate electric fields at very small tip-sample distances in atomic force microscopy," *Applied Physics Letters*, vol. 97, no. 3, p. 033115, Jul 2010.

[26] Z. Wei, R. Chen, and X. Chen, "Nonlinear reconstruction of multilayer media in scanning microwave microscopy," *IEEE Transactions on Instrumentation and Measurement*, vol. 68, no. 1, pp. 197–205, May 2019.

[27] G. M. Sacha, C. Gómez-Navarro, J. J. Sáenz, and J. Gómez-Herrero, "Quantitative theory for the imaging of conducting objects in electrostatic force microscopy," *Applied Physics Letters*, vol. 89, no. 17, p. 173122, Oct 2006.

[28] A. A. Chlenova, A. A. Moiseev, M. S. Derevyanko, A. V. Semirov, V. N. Lepalovsky, and G. V. Kurlyandskaya, "Permalloy-based thin film structures: Magnetic properties and the giant magnetoimpedance effect in the temperature range important for biomedical applications," *Sensors*, vol. 17, no. 8, Aug 2017.

[29] L. Lu, "Damping mechanisms in magnetic recording materials microwave-assisted magnetization reversal," Ph.D. dissertation, Dept. Physics, Colorado State Univ., Colorado, CO, USA, 2014.

[30] P. Wang, N. Tien, and E.-C. Kan, "Permalloy loaded transmission lines for high-speed interconnect applications," *IEEE Transactions on Electron Devices*, vol. 51, no. 1, pp. 74–82, Jan 2004.

[31] M. Aldrigo, A. Cismaru, M. Dragoman, S. Iordanescu, E. Proietti, G. M. Sardi, G. Bartolucci, and R. Marcelli, "Amplitude and phase tuning of microwave signals in magnetically biased permalloy structures," *IEEE Access*, vol. 8, pp. 190 843–190 854, Oct 2020.

[32] G. M. Sardi, A. Lucibello, M. Kasper, G. Gramse, E. Proietti, F. Kienberger, and R. Marcelli, "Optimization of the imaging response of scanning microwave microscopy measurements," *Applied Physics Letters*, vol. 107, no. 3, p. 033107, Jul 2015.

[33] B. Lax and K. J. Button, *Microwave Ferrites and Ferrimagnetics*. Newyork: Mc-Graw-Hill, 1962, chapter 4, pp. 145–189.

[34] C. Kittel, "On the theory of ferromagnetic resonance absorption," *Phys. Rev.*, vol. 73, pp. 155–161, Jan 1948.

[35] C. Wang, H. Seinige, and M. Tsoi, "Ferromagnetic resonance driven by an ac current: A brief review," *Low Temperature Physics*, vol. 39, no. 3, pp. 247–251, Mar 2013.

[36] M. Wu and A. Hoffmann, *Recent Advances in Magnetic Insulators – From Spintronics to Microwave Applications*, 1st ed. Special Issue of Solid State Physics, Oct 2013, pp. 1–392.

[37] T. Edwards, *Foundations for Microstrip Circuit Design*, 2nd ed. John Wiley and Sons, Newyork, 1992.

[38] A. Ganguly and D. Webb, "Microstrip excitation of magnetostatic surface waves: Theory and experiment," *IEEE Transactions on Microwave Theory and Techniques*, vol. 23, no. 12, pp. 998–1006, Dec 1975.

[39] P. Kabos and V. S. Stalmachov, *Magnetostatic Waves and Their Application*, 1st ed. Springer, Dordrecht, 1994.

[40] R. Marcelli, G. Sajin, A. Cismaru, and F. Craciunoiu, "Band-stop magnetostatic waves micromachined resonators," *Applied Physics Letters*, vol. 84, no. 13, pp. 2445–2447, Mar 2004.

[41] G. Bartolucci and R. Marcelli, "A generalized lumped element modeling of magnetostatic wave resonators," *Journal of Applied Physics*, vol. 87, no. 9, pp. 6905–6907, Apr 2000.

[42] R. Marcelli, E. Andreta, G. Bartolucci, M. Cicolani, and A. Frattini, "A magnetostatic wave oscillator for data relay satellite," *IEEE Transactions on Magnetics*, vol. 36, no. 5, pp. 3488–3490, Sep 2000.

[43] H. Tanbakuchi, M. Richter, F. Kienberger, and H.-P. Huber, "Nanoscale materials and device characterization via a scanning microwave microscope," in *IEEE International Conference on Microwaves, Communications, Antennas and Electronics Systems*, 2009, pp. 1–4.

[44] H. P. Huber, I. Humer, M. Hochleitner, M. Fenner, M. Moertelmaier, C. Rankl, A. Imtiaz, T. M. Wallis, H. Tanbakuchi, P. Hinterdorfer, P. Kabos, J. Smoliner, J. J. Kopanski, and F. Kienberger, "Calibrated nanoscale dopant profiling using a scanning microwave microscope," *Journal of Applied Physics*, vol. 111, no. 1, p. 014301, Jan 2012.

[45] H. Chen, P. De Gasperis, and R. Marcelli, "Using microwave network analyzer and msw-ser to measure linewidth spectrum in magnetic garnet film from 0.5 to 20 ghz," *IEEE Transactions on Magnetics*, vol. 29, no. 6, pp. 3013–3015, Nov 1993.

[46] S. Tamaru, S. Tsunegi, H. Kubota, and S. Yuasa, "Vector network analyzer ferromagnetic resonance spectrometer with field differential detection," *Review of Scientific Instruments*, vol. 89, no. 5, p. 053901, May 2018.

[47] L. Michalas, E. Brinciotti, A. Lucibello, G. Gramse, C. H. Joseph, F. Kienberger, E. Proietti, and R. Marcelli, "De-embedding techniques for nanoscale characterization of semiconductors by scanning microwave microscopy," *Microelectronic Engineering*, vol. 159, pp. 64–69, Jun 2016.

C. H. Joseph received BSc degree in physics from St. John's College, Tirunelveli, India and MSc degree in physics from The American College, Madurai, India. From 2010 to 2013, he worked as a project associate at the Microwave laboratory, Department of Physics, Indian Institute of Technology Madras, India. In 2013, he received European Commission's Marie Curie ITN Research Fellowship and joined as an ESR at CNR-IMM Rome unit and received his Ph.D. degree in Electronics Engineering from University of Rome Tor Vergata, Italy in 2016. From 2017 to 2018, he worked as a post-doctoral researcher at the Department of Physics, IIT Madras, India. He is currently working as a researcher at the Department of Information Engineering, Università Politecnica delle Marche, Italy. His current research interest includes nanoscale characterization of 2D advanced materials and biological structures using Scanning Microwave Microscopy technique, Nanoelectronics, Microwave/mm wave metamaterials device modelling and design.

Georg Gramse is Scientific Researcher at Keysight Technologies and group leader of the Nanoelectronics group at Johannes Kepler University Linz. He studied Physics at Freie University Berlin and Nanotechnology at University of Barcelona. He received his PhD in Nanoscience at the University of Barcelona and IBEC and has a strong expertise in electrical metrology at the nanoscale based on scanning probe microscopy and other characterization techniques. He developed new electrical measurement techniques/ methods and applied them to solve open research questions in various fields like Biophysics, Electrochemistry, Material Science and Semiconductor-Physics giving rise to publications in Science and Nature journals. The special technological emphasis on broad frequency and high-speed electrical measurements at the nanoscale is combined with the development of accurate and numerical quantification procedures based on finite element modelling.

Emanuela Proietti received the degree in electronic engineering, in 1996. From 1996 to 2000, she worked as the Clean Room Lead Engineer in Texas Instruments Italia, Avezzano Semiconductor Plant. In 2000, she joined the ALCATEL Italia, Rieti plant, as the Maintenance Director for Surface Mount Technology assembly production equipment. In 2001, she joined CNR-Institute for Microelectronics and Microsystems Rome as a Research Engineer. From 2005 to 2014, she was the Clean Room Area Coordinator of the IMM-Roma institute. She has served as the coordinator/team member of several national and international projects. Her current scientific interests include RF-MEMS devices, polymeric-based RF devices and membrane, meta-structured devices for microwave and Microwave Microscopy and Tomography applied to Cultural Heritage.

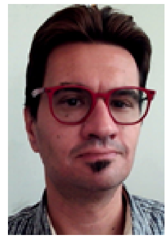

Giovanni Maria Sardi (Member, IEEE) was born in Siena, Italy, in 1980. He received the M.Sc. degree in telecommunication engineering and the Ph.D. degrees in information engineering (curricula for electromagnetic waves engineering) from the University of Siena, in 2008 and 2012, respectively. He is currently a Researcher with the Institute for Microelectronics and Microsystems, National Research Council of Italy, Rome (CNR-IMM). He has published articles in various conferences and journals. His main research topics are design, modeling, and testing of radio-frequency devices for telecommunications and sensing. He is also interested in microwave microscopy applications and applied electromagnetics theory. He serves as a reviewer for journals and as a TPC member in conferences about antennas, microwave devices, and high-frequency sensors. He thanks the Precari Uniti CNR Association for the support in conducting his research activity.

Gavin W. Morley leads a research group in the Warwick University Physics Department. He did an undergraduate degree and a PhD in Physics at Oxford University. He has held fellowships from the 1851 Royal Commission and the Royal Society, as well as being supported by three of the UK Quantum Technology Hubs. His research group builds quantum experiments and technologies based on nitrogen vacancy colour centres in diamond. This includes magnetometry, quantum computing chips and an experiment with a levitated nanodiamond which aims to put the nanodiamond into a spatial quantum superposition. In time this may permit a test of quantum gravity.

Ferry Kienberger received the Ph.D. degree in technical physics and the Habilitation degree in nanotechnology from the Technical Faculty, JKU Linz, in 2002 and 2019, respectively. He is Keysight Austria Country Manager and Keysight Laboratories Linz Group Leader on battery science. Prior to this, he was a Scientist at Agilent Technologies working on nanotechnology. The scientific track record includes more than 120 scientific peer-reviewed publications (including the Nature Publishing Group and Science Advance) with an H-factor 40 and 5000+ citations; he supervised ten Ph.D. theses. He was the lead partner in more than 15 EU projects for Keysight and Agilent, 7 national projects, 2 international projects (Economic Development Board Singapore), and 3 metrology EU projects. He serves as the Vice-Chair for the EU H2020 Program and is a former member of the Organisation for Economic Co-operation and Development (OECD) Business and Industry Advisory Council (BIAC) for Nanotechnology.

Giancarlo Bartolucci graduated from the University of Roma La Sapienza in 1982 with a thesis on integrated optics. In 1982 he was with the "Fondazione Ugo Bordoni", Roma. In 1983 he served as officer in the Technical Corps of the Army. In 1984 he became a Reseacher at the Department of Electronic Engineering of the University of Roma "Tor Vergata". From 1992 to 2013 he was Associate Professor of Microwave Integrated Circuits in the same Department. He is currently Associate Professor of High Frequency Distributed Circuits. He conducted research on the modelling of microstrip and coplanar passive components. In recent years, he was working on design methods of distributed phase shifters and amplifiers. His research interests include the development of equivalent circuits for RF MEMS devices, and their use for the design of switches and phase shifters. He is active also in the field of metamaterials for microwave and millimetre wave applications.

Romolo Marcelli was born in Roma, Italy, on February 26, 1958. He obtained the degree in Physics at the University of Roma ”La Sapienza” in 1983. From 1987 he is with the National Research Council (CNR) of Italy, and from 1998 with the Institute for Microelectronics and Microsystems (IMM) of CNR. Presently, he is a Senior Researcher and Responsible of the Research Line on “High Frequency Microsystems: Technologies and Reliability for Ground and Space Applications at CNR-IMM Roma”. His past and current interests include technologies, design and test activities in Microwave Magnetics and RF MEMS. Currently, he is also involved in Microwave Imaging and Metamaterials at Microwave and Millimeter Wave Frequencies. In this framework, he also managed several national and international industrial and academic contracts, and he served as organizer and committee member in workshops and conferences. He is Editor of two books on the linear and non-linear properties of magnetic microwave devices, and co-author of more than two hundred international papers and conference contributions on microwave magnetic devices, RF MEMS and Microwave Scanning Microscopy.